Dynamic Behavior of Vortex Rings and Characteristics of Dynamic Forces Formed by Elastic Butterfly Wing

S. Haishi[1]* and M. Fuchiwaki[1]

1: Graduate School of Computer Science and Systems Engineering, Major of Creative Informatics
Kyushu Institute of Technology, Japan

* Correspondent author: haishi.sei211@mail.kyutech.jp

Abstract

Recently, membrane airfoil which is inspired from the butterfly and bat wing is researched the flow field and dynamic fluid forces generated by the motion of wing. Authors investigated 3D shape of wing and dynamic behavior of vortex rings because the butterfly wing demonstrates the high performance by only flapping motion and elastic deformation of wing. In this study, For clarifying the dynamic behavior of vortex rings and characteristics of fluid forces, we implemented the simultaneous measurement of flow field and lift generated by the flapping motion of butterfly wing. On the both of downstroke and upstroke, the amplitude of maximum velocity of vortex core increase after the elastic deformation of wing is happened. That elastic deformation is occurred by the maximum dynamic lift on each stroke. Especially, the maximum velocity of wing tip vortex core is the most developed after the elastic deformation of butterfly wing on both stroke.

Keyword: *Wake, Vortex ring, Vortex core, Membrane airfoil, Butterfly wing*

1. Introduction

An object with elastic deformation generates a vortex ring in the surrounding fluid when it moves in fluid. The behavior of the vortex ring changes with not only the motion of the object (velocity, acceleration) but also the shape of the object (thickness, edge shape, camber). In particular, the behavior of the vortex ring changes unsteadily because the elastic airfoil always deforms during the motion. Although this phenomenon is very unsteady, the elastic moving airfoil is expected to be used for the industrial application of flying robots and MAVs because it provides a higher performance than a rigid moving airfoil[1,2]. In particular, a creature that flies or swims in a fluid uses its elastic airfoil (wing or fin) very effectively. Therefore, for the purpose of clarifying the mechanism of demonstrating the high performance of the elastic airfoil, the wake that is generated by using an organ such as a wing and or fin during motion has been investigated extensively[3-6].

Recently, the very-thin-membrane airfoil has been determined to be attractive in terms of the design and development of flying robots, such as those intended for use on Mars, and robustness to sudden disturbances of flying robots, such as those intended for use on Mars, and robustness to sudden disturbances. This membrane airfoil is inspired by flying creatures such as butterflies and bats, and the flow field generated by the motion of the elastic airfoil has been clarified. A wing of a butterfly controls its flow field with not only its elastic deformation and oscillation: the flow field depends on all the motion of the airfoil. On the other hand, a butterfly demonstrates high flight performance with only the motion and elastic deformation of airfoils because the flapping frequency and natural frequency of the wings are different[7]. The camber of a butterfly wing is useful for generating dynamic lift and forming a well-developed vortex ring during flapping motion[8]. The author focused on this flapping motion of a butterfly wing as an application of the wing[9]. Membrane airfoil and clarified the dynamic behavior of vortex rings in the wake[9] and elastic deformation of the wing[10]. Although we have clarified the deformation of the butterfly wing and the dynamic behavior of vortex rings during flapping motion of the wing, which part of the vortex ring is developed relative to the quantitative wing phase has not yet been sufficiently clarified. In addition, the change in dynamic lift as the vortex ring develops is also unclear, and the relationship between the dynamic behavior of the vortex ring is developed relative to the quantitative wing phase has not yet been sufficiently clarified. In addition, the change in dynamic lift as the vortex ring develops is also unclear, and the relationship between the dynamic behavior of the vortex ring

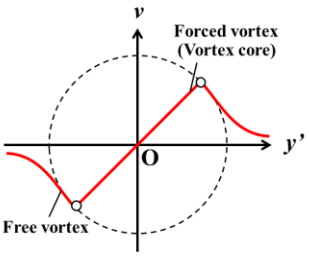

Fig. 1 Velocity distribution of vortex core

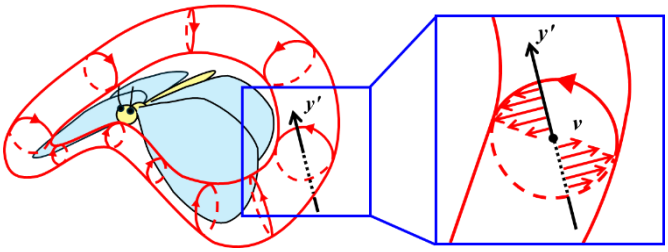

Fig. 2 Setting the axis for measuring the velocity of vortex core

generated by the flapping motion of the wings of a butterfly and the unsteady lift also not been clarified.

The purpose of the present study is to clarify the dynamic behavior of vortex rings and the characteristics of dynamic lift generated by the flapping motion of an elastic butterfly wing, which is an example of a membrane airfoil. In particular, we visualize the vortex rings generated by the flapping motion equivalent to take off flight from two directions by 2DPIV measurement and determine the change in scale and velocity of the vortex core of the vortex ring. Moreover, the vortex core, we will clarify the dynamic behavior of the vortex ring related to the generation of dynamic lift.

2. Material and Methods

2.1 Experimental setup

In the present study, we used *Idea leuconoe* as the experimental subject and measured the flow field and dynamic lift generated by the flapping motion of a butterfly wing. It is difficult to measure the vortex ring and dynamic lift generated by the flapping motion when a butterfly performs free flight because the direction of flight is unsteady. Therefore, the legs of the butterfly were fixed to the tip of a shaft and measurements were taken while the butterfly was performing a flapping motion similar to take-off flight[9,10]. Visualization measurements were implemented at three positions: the leading edge, the trailing edge, and the wing tip. In measurements, the flapping angle φ of the wings of the butterfly was calculated from the three-dimensional positions of the wings tips obtained from two orthogonal high-speed cameras (Photoron, Limited FASTCAM SA-X2)[11] and used as the wing phase. For a given flapping angle φ, the vortices at the leading edge, trailing edge, and tip of the wing are always generated in the same way regardless of time or individual butterfly. Moreover, we measured the dynamic lift generated by the flapping motion using a small six-axis sensor (BL Autotec, NANO 1.2/1-A-R) synchronized with two high-speed cameras. In order to easily grasp the change in dynamic lift, the change in the measured valued was used.

2.2 Vortex core

There are methods for extracting the vortex from a rotating flow, using factors such as vorticity and Q value[12,13]. However, it is difficult to grasp the outline of the vortex core because the vorticity extracts even shear flow as high vorticity. Although Q value can also extract the rotating component from the flow field using the tensor, the size of the extracted region changes depending on the set value, so the vortex core cannot be clearly captured. Thus, in the present study, we used the velocity distribution measured from the rotating flow generated by the flapping motion of a butterfly wing. Fig. 1 shows a schematic diagram of the velocity distribution of the vortex. As shown in this figure, velocity changes linearly with distance from the center of the vortex in the forced vortex, and velocity changes inversely proportional to the distance from the center of the vortex. In this velocity distribution, we regarded the region between the positive and negative maximum velocities in the forced vortex as the vortex core[3]. We will clarify the change in scale (the distance between the positive and negative maximum velocities is regarded as the diameter of the vortex core) and velocity distribution from the visualization results. Fig. 2 shows a representation of the axis for measuring the velocity of the vortex core. As shown in this figure, the axis runs through the center of the vortex of the vortex ring generated by the flapping motion of the butterfly wing. Moreover, we measured the velocity distributions of three vortex cores: the leading edge vortex, the trailing edge vortex, and the wing tip vortex. The direction of vortex pairs measured form the visualize measurements. In the present study, we assumed that the flow field generated by the flapping motions of a pair of butterfly wings are symmetric when measuring the scale and velocity distribution of the vortex core. Therefore, we measured the leading edge vortex, the trailing edge vortex, and the wing tip vortex generated by the flapping motion of the left wing. Based on these results, we

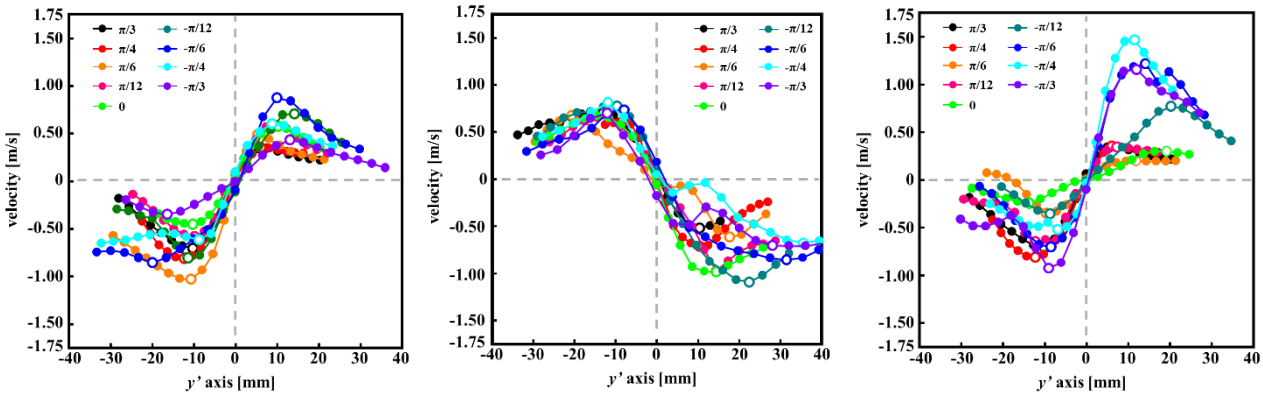

(a) Leading edge vortex (b) Trailing edge vortex (c) Wing tip vortex

Fig. 3 Velocity distribution of vortex core on downstroke

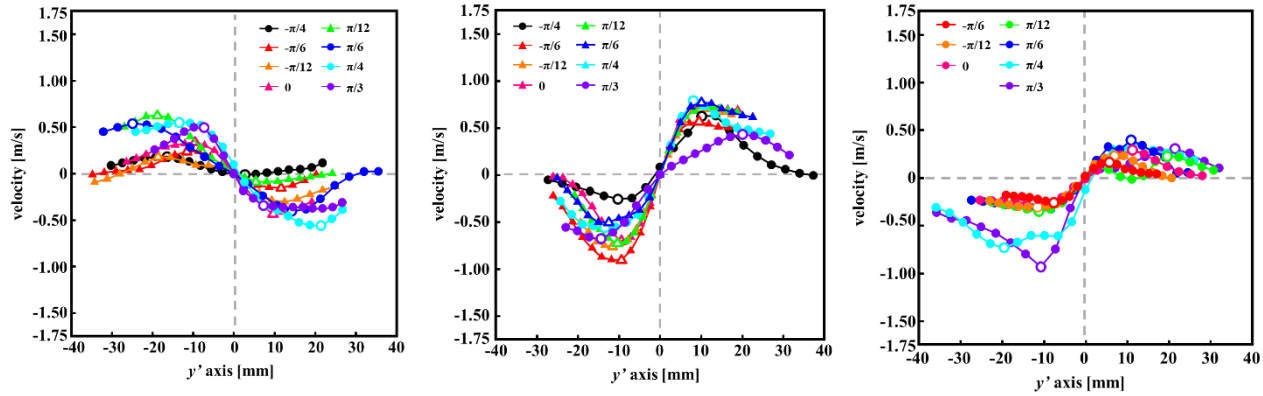

(a) Leading edge vortex (b) Trailing edge vortex (c) Wing tip vortex

Fig. 4 Velocity distribution of vortex core on upstroke

determine the change in scale and the velocity distributions of the vortex core relative as the change of the wing phase. Furthermore, we will also clarify the behavior of the vortex core relative to the dynamic lift by comparing the dynamic lift with the wing phase.

3. Results and discussion

Fig. 3 is the velocity distribution of vortex core based on the wing phase during downstroke of the wing. Fig. 3(a), (b), and (c) show the velocity distribution of the leading edge vortex, the trailing edge vortex, and the wing tip vortex. The colors in Fig. 3 are the results for different wing phases (black: π/3 rad, red: π/4 rad, orange: π/6 rad, pink: π/12 rad, yellow green: 0 rad, green: -π/12 rad, blue: -π/6 rad, sky blue: -π/4 rad, and purple: -π/3 rad). And, the range of the results is φ = π/2 to -π/3 rad because the bottom dead position is φ = -π/3 rad. Moreover, the hollow points are the positions of the maximum velocity of the vortex core in the figure.

As shown in Fig. 3(a), although the positive maximum velocity of the leading edge vortex, the negative maximum velocity increases before the wing passes the horizontal position. Both signs of maximum velocity become approximately 0.75 m/s after the wing passes the horizontal position (green: φ = -π/12 rad). As the downstroke of the wing continues, the maximum velocity of the vortex core decreases gradually. When the wing reaches the bottom dead position (purple: φ = -π/3 rad), the maximum velocity become approximately 0.5 m/s. In addition, regarding the scale of vortex core, although it is approximately 15 mm at the beginning of the downstroke (black: φ = π/3 rad), it enlarges to approximately 25 mm after the wing passes through the horizontal position (green: φ = -π/12 rad). Then, it further expands to approximately 30 mm when the wing reached the bottom dead position (blue: φ = -π/6 rad). The scale of the vortex core remains approximately constant until the wing reached the bottom dead position (purple: φ = -π/3 rad).

At the trailing edge vortex (Fig. 3(b)), the position of negative maximum velocity of the vortex core is far from the center of the vortex and is very far from -0.5 to -1.0 m/s (φ = π/6 to -π/3 rad). However, the position of positive maximum velocity hardly changes, and the maximum velocity value remains about 0.75 m/s.

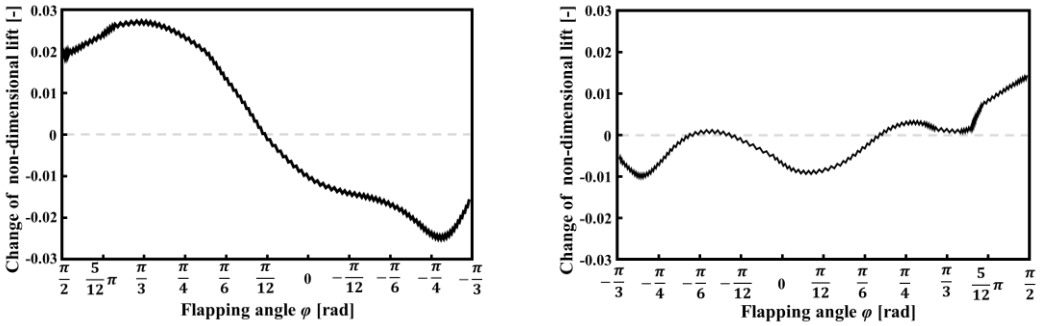

(a) Downstroke (b) Upstroke

Fig. 5 Change of non-dimensional lift generated by flapping motion

At the wing tip vortex (Fig. 3(c)), neither the positive nor negative maximum velocity of the vortex core develops, and instead they both decrease until the wing passes through the horizontal position (φ = 0 rad). However, after the wing passes the horizontal position (green: φ = -π/12 rad), the positive maximum velocity dramatically increases as the downstroke continues. In particular, the positive maximum velocity increases to approximately 1.5 m/s (sky blue: φ = -π/4 rad). Moreover, the maximum velocity does not decrease dramatically even when the wing reaches the bottom dead position (purple: φ = -π/3 rad). Although the positive maximum value is slightly larger than the negative maximum velocity, both values are approximately 1.0 m/s. The position of maximum velocity of the vortex core changes only slightly and diameter remains at approximately 20 mm after the wing passes through the horizontal position (φ < -π/12 rad).

The reason why the negative maximum velocity of the trailing edge vortex behaves differently from the other two vortices is thought to be due to the positional relationship between the vortex core and the edge of the wing. The leading edge vortex generated by the downstroke of the wing attaches to the leading edge and becomes steady as a result of the axial flow[14]; after the scale of vortex core expands, it maintains a roughly constant scale. In addition, although the position fluctuates, no large change in the position is observed because the wing tip vortex does not separate from the edge of the wing. On the other hand, the trailing edge vortex separates from the trailing edge as the phase of the wing progresses with the downstroke. Therefore, there is no supply of the flow on the wing surface during the downstroke to trailing edge vortex, and, as a result, the maximum negative velocity of the vortex core, which moves away from the induced flow between the vortex pair, gradually decays as its position changes due to interaction with the surrounding fluid.

In addition, the maximum velocity of the wing tip vortex, in other words, the increase in the velocity of the upper part of the vortex ring at the wing tip, is characteristic. The other two vortexes expand the scale and increase the vortex gradually. However, the increase in the positive maximum velocity more dramatically expands the scale of the vortex core. Therefore, we thought that the vortex core rolled up from the wing tip developed without expanding the scale of vortex core, but the velocity of the flow was increased by the vortex. In the present study, the visualization plane in the wingspan direction is set to pass through the thorax of the butterfly[10]. In the downstroke of the wing, the butterfly makes the wing tip move forward slightly[9]. Thus, in the visualization plane that was set, the vortex that rolled up at the wing tip was measured not from a fixed point on the wing, but moving from the front of the wing tip to the rear of the wing tip. In previous research, the vortex ring was generated by the downstroke of the wing. At the beginning of the downstroke of the wing, the maximum vorticity was located at the wing tip of the forewing. When the wing approaches the bottom dead position, this position moves to the wing tup of the hindwing[9]. In the present study, when the wing reaches the bottom dead position (purple: φ = -π/3 rad), the position of the visualization plane is near the wing tip of the hindwing. Although the measurement result is the velocity distribution of the vortex core, this result is valid because we determine the development of the vortex ring on the downstroke.

Fig. 4 shows the velocity distribution of the vortex core generated by the upstroke. Fig. 4(a), (b), and (c) represent the results for the leading edge vortex, the trailing edge vortex, and the wing tip vortex, respectively. The colors in Fig. 4 indicate the results for each wing phase (black: -π/4 rad, red: -π/6 rad, orange: -π/12 rad, pink: 0 rad, yellow green: π/12 rad, blue: π/6 rad, sky blue: π/4 rad, and purple: π/3 rad). The results shown in Fig. 4 were obtained after the rotating flow became visible on the visualization planes (leading edge, trailing edge: φ > -π/4 rad, Fig. 4(a) and (b); wing tip: φ > -π/6 rad, Fig. 4(c)). Due to the induced flow inside the vortex ring generated by the downstroke, the velocity distribution of the vortex core generated by the upstroke did not have a central velocity of 0, but there were results in which the velocity distribution had two inflection

points. Therefore, in order to grasp the scale and velocity distribution of the vortex core, the center of the vortex core was set at 0 by subtracting the velocity of the vortex core. These results are indicated by triangles in Fig. 4. Moreover, hollow points represent both the downstroke and the position of the maximum velocity of the vortex core.

The positive maximum velocity of the vortex core of the leading edge vortex increases as the wing phase increases as the downstroke continues (Fig. 4(a)). However, even the largest velocity of the vortex core (approximately 0.5 m/s) is slower than the leading edge vortex of the downstroke. Moreover, the fluctuation of the vortex core scale is very large. Although the scale of the vortex core is approximately 20 mm (φ = -π/4 to -π/6 rad) at the beginning of the upstroke, it increases to approximately 40 mm after the wing passes through the horizontal position (φ = π/6 to π/4 rad). Then, as the upstroke progress, the scale of the vortex core shrinks to approximately 20 mm as the wing reaches the top dead position (φ = π/3 rad). The vortex core of the trailing edge vortex is slightly larger, and the velocity distribution is developed than those of leading edge vortex. However, like the leading edge vortex on the upstroke, since the velocity distribution of the vortex core is smaller than that of the trailing edge vortex downstroke on the trailing edge, it does not develop. Moreover, the maximum velocity of the vortex core of the wing tip vortex is smaller than that of the downstroke (Fig. 4(c)). From the results for the velocity distribution, the velocity of the vortex core generated by the upstroke do not develop than those of the downstroke.

However, the velocity distribution of the wing tip vortex showed quantitatively the same tendency as that of the wing tip vortex generated by downstroke. Until just after the wing passes the horizontal position (φ = -π/4 to π/12 rad), there is no large change in velocity, and the scale of vortex core (diameter) only increases. On the other hand, the negative maximum velocity of the vortex core, that is, the lower part of the vortex core, increases to approximately -1.0 m/s as the upstroke progresses (φ = π/4 to π/3 rad). From these results, in either downstroke or upstroke, the behavior of the wing tip vortex is different from other vortexes. Although the scale of vortex core expands, it remains constant until the wing passes through the horizontal position. After that, it is thought that the vortex then develops by increasing its velocity at the upper part of the vortex on downstroke and at the lower part of the vortex on upstroke. In addition, we expect that the velocity of the developed vortex core of the wing tip vortex contributes to the acceleration of the induced flow in the vortex ring.

The scale and velocity distribution of vortex core indicated the behavior of the vortex core on the downstroke and upstroke of wing. In response to these changes, by comparing the change in dynamic lift generated by each stroke, we will clarify the behavior of the vortex ring related to the generation of the dynamic lift.

Fig. 5 shows the change in dynamic lift generated by the flapping motion of the butterfly wing relative to the wing phase. Fig. 5(a) and (b) represent the results for the downstroke and upstroke, respectively. The range of results in Fig. 5, similar to the results for the velocity and scale of the vortex core, is φ = -π/3 to π/2 rad. In the figure, the dynamic lift is non-dimensionalised by the mass of the butterfly.

As shown in Fig. 5(a), the dynamic lift is most increased at the beginning of the downstroke (φ = π/2 to π/3 rad). Then, the amount of increase in dynamic lift becomes 0, the dynamic lift becomes maximum before the wing passes through the horizontal position.

Since the change in dynamic lift generated by the upstroke (Fig. 5(b)) varied from a negative value until φ = π/4 rad to a positive value, the negative maximum value of the dynamic lift is generated after the wing passes through the horizontal position. Although the change in the unsteady lift generated by the downstroke remains negative for a longer period of time, the magnitude of this change is small, so it is thought that the dynamic lift generated by the upstroke is smaller than that generated by the downstroke.

The increase in the maximum velocity of the vortex core generated at each position is delayed in wing phase with respect to this change in dynamic lift. As shown in Fig. 3(a), (b), and (c), the maximum velocity of the vortex core at any position dramatically increases when the wing is located near the horizontal position (φ = 0 rad) on the downstroke. In addition, on the upstroke, the increase in the maximum velocity of the vortex core occurs near φ = π/6 rad when the negative dynamic lift becomes approximately maximum. In particular, the negative maximum velocity of the vortex core at the wing tip increases after φ = π/4 rad, so that the wing phase is delayed compared to the other position (φ = π/6 rad). Therefore, during either the downstroke or the upstroke of the wing, the maximum velocity of the vortex core increases after the dynamic lift becomes maximum.

These changes likely occur in conjunction with the elastic deformation of the butterfly wing. On the downstroke, when the wing passes through the horizontal position (φ = 0 rad), the wing deforms into an arch shape. The deformation then becomes larger[10]. Since the dynamic lift begins to decrease when the wing reaches the horizontal position (φ = 0 rad), the elastic deformation is thought to have occurred after the dynamic lift becomes maximum. The maximum velocity of the vortex core, in particular, that of the wing tip

vortex, dramatically increases after the wing passes through the horizontal position. On the other hand, on the upstroke, the elastic deformation of the butterfly wing happened after the wing passes through the horizontal position ($\varphi = \pi/6$ rad)[10], which is when the negative dynamic lift becomes maximum. Accordingly, the maximum velocity of the vortex core dramatically increases after elastic deformation of the wing occurs ($\varphi > \pi/6$ rad). As such, the maximum velocity of the vortex core of the wing tup vortex increases after elastic deformation of the wing occurs. This deformation promotes the increase of the velocity after generation of the maximum dynamic lift.

Based on these results, we clarified the dynamic behavior of the vortex rings and the dynamic lift generated by flapping motion of a butterfly wing. On the downstroke, before the wing passes through the horizontal position, the dynamic lift becomes maximum. After that, elastic deformation of the butterfly wing occurs, and, in conjunction, the velocity of the upper part of the vortex core increases dramatically. Moreover, on the upstroke, the negative dynamic lift becomes maximum with elastic deformation of the wing. The maximum velocity of the vortex core on both strokes is the elastic deformation of the butterfly wing due to the maximum dynamic lift.

4. Conclusion

The dynamic behavior of the vortex rings and the characteristics of dynamic lift generated by the flapping motion of the butterfly wing as an application of ta membrane airfoil are clarified. On either stroke, the elastic deformation of the wing occurred after the maximum lift was generated. In addition, although there is a difference of wing phase in the elastic deformation of the wing, after the elastic deformation of the wing, the maximum velocity of the vortex core increases. In particular, at the wing tip, the maximums at the top the vortex on the downstroke and at the bottom of the vortex on the upstroke are thought to dramatically increase.

References

[1] Ashraf, A. M., Young, J. and Lai, J. C. S., “Reynolds number, thickness and camber effects on flapping airfoil propulsion”, *Journal of Fluids and Structures*, Vol. 27 No. 2 pp.145-160(2011): DOI 10.1016/j.jfluidstructs.2010.11.010

[2] Jaworski, W. J. and Gordnier, E. R., Thrust augmentation of flapping airfoils in low Reynolds number flow using a flexible membrane, Journal of Fluids and Structures, Vol.52, (2015), pp.199-209

[3] Drucker, E. G. and Lauder, G. V., “Locomotor forces on a swimming fish three-dimensional vortex wake dynamics quantified using digital particle image velocimetry”, *Journal of Experimental Biology*, Vol. 202 (1999): pp.2393-2412. DOI https://doi.org/10.1242/jeb.202.18.2393

[4] Drucker, E. G. and Lauder, G. V., “A hydrodynamic analysis of fish swimming speed wake structure and locomotor force in slow and fast labriform swimmers”, *Journal of Experimental Biology*, Vol. 203 (2000): pp.2379-2393. DOI https://doi.org/10.1242/jeb.203.16.2379

[5] Drucker, E. G. and Lauder, G. V., “Wake dynamics and fluid forces of turning maneuvers in sunfish”, *Journal of Experimental Biology*, Vol. 204 (2001): pp.431-442 DOI https://doi.org/10.1242/jeb.204.3.431

[6] Gemmell, B. J., Troolin, D. R., Costello, J. H., Colin, S. P., and Satterlie, R. A. “Control of vortex rings for manoeuverability”, *Journal of The Royal Society Interface*, 12(108), (2015): DOI https://doi.org/10.1098/rsif.2015.0389

[7] Shen, H., Ji, A., Li, Q., X., and Ma, Y., “Tensile mechanical properties and finite element simulation of the wings of the butterfly Tirumula limniace”, *Journal of Comparative Phycology A*, 209(2), pp.239-251(2023)

[8] Fang, Y. H., Tang, C. H., Lin, Y. J., Yeh, S. I. and Yang, J. T., “The lift effects of chord wise wing deformation and body angle on low-speed flying butterflies”, *Biomimetics*, 8(3), 287, (2023): DOI 10.3390/biomimetics8030287

[9] Fuchiwaki, M., Kuroki, T., Tanaka, K. and Tabata, T., “Dynamic behaviour of the vortex ring formed on a butterfly wing”, Experimental in Fluids, Vol. 54 No. 1450(2013): DOI 10.1007/s00348-012-1450-x

[10] Haishi, S. and Fuchiwaki, M., “Dynamic behavior of two-pairs of vortices rolled up from elastic butterfly wings”, *Proceedings of the ASME2024 Fluids Engineering Division Summer Meeting*. FEDSM2024-130889

[11] Sunada, S., Kawachi, K., Watanabe, I. and Azuma, A., “Performance of a butterfly in take-off flight”, *Journal of Experimental Biology*, Vol. 183 No. 1 pp.249-277(1993): DOI https://doi.org/10.1242/jeb.183.1.249

[12] Chen, Q., Zhong, Q., Qi, M. and Wang, X., “Comparison of vortex identification criteria for planar velocity fields in wall turbulence”, *Physics of Fluids*, Vol. 27 No. 8(2015): DOI https://doi.org/10.1063/1.4927647

[13] Jeong, J. and Hussain, F., “On the identification of a vortex”, *Journal of Fluid Mechanics*, Vol.285 pp.69-94(1995): DOI 10.1017/S0022112095000462

[14] Van Den Berg, C. and Ellington, C. P., “The vortex wake of a ‘hovering model hawkmoth”, *Philosophical Transactions of the Royal Society of London. Series B: Biological Sciences*, 352(1351), pp.317-328(1997)